

**PRECISE AND RAPID CALCULATIONS OF ENERGY AND PARTICLE FLUX  
FOR DETAILED BALANCE PHOTOVOLTAIC APPLICATIONS**

M.Y. Levy and C. Honsberg

Department of Electrical and Computer Engineering, University of Delaware;  
140 Evans Hall; Newark, Delaware 19716, U.S.A.  
e-mail: mlevy@ece.gatech.edu

**ABSTRACT:** The central problem that this paper addresses is the rapid and precise calculation of the energy and particle flux for photovoltaic efficiency limit calculations. The calculation of energy and particle flux is essential to modeling the efficiency limits of solar energy conversion. Computing flux with the canonical Bose-Einstein integral is time consuming and, without due care, prone to error. The approach given herein, transforms the Bose-Einstein integral into a linear combination of incomplete Riemann zeta integrals. The numerical package that implements this method is benchmarked for precision by a number of means. These include comparisons between the Riemann zeta functions, and previously recorded values of solar cell limiting efficiencies from the literature. The numerical package is used to compute the optimized efficiencies of the intermediate band solar cell for solar concentrations intermediate between the two extreme values.

**Keywords:** Fundamentals, High-Efficiency, Solar Cell Efficiencies

## 1 INTRODUCTION

The calculation of energy and particle flux is essential to modeling the efficiency of solar energy conversion. This is irrespective of whether detail-balance or thermodynamic calculations are employed. Additionally, such calculations are made when modeling the efficiency limits of a wide variety of energy converters, such as thermophotovoltaic devices [1]. Though efficiency limit modeling has been undertaken for decades [2], some of the advanced photovoltaic concepts that have arisen have stimulated the present day demand for higher performance methods to calculate flux. For example, efficiency limit calculations for solar energy applications with internal constraints placed upon the generation or recombination flux (e.g. IBSC, serial-connected tandem) require many calculations just to satisfy the constraints, and hence are very time intensive. Further bolstering the demand for higher performance methods, are applications where it is necessary to calculate the flux when the chemical potential of the photons is very near to the band gap of the converter. In such cases, the calculation of flux requires the evaluation near a singularity (c.f. Eq. 1, which has a singularity as  $\mu$  approaches  $E_A$ ). A high performance method for calculating flux is obtained by transforming the canonical forms of the flux into a linear combination of integrals, whose integrands are functions of a single dummy variable. Look-up-tables (LUT) may then be computed over the domain of the dummy variable.

Flux is written canonically as a Bose-Einstein integral, which has no closed form solution. Therefore, some combination of numerical methods, expansions [3,4,5], and limiting expressions are required to evaluate flux. As regards numerical methods, numerically integrating the Bose-Einstein integral is time consuming and, without due care, prone to error. The errors largely derive from the limited degree of accuracy of numerical integration routines and the high order interpolation needed to fit the spectrum of the radiation. When modeling the efficiency limits of devices with internal constraints the speed of computation is placed at a premium and the use of the Bose-Einstein becomes unsatisfactory. For example, in modeling the efficiency limit of an IBSC, the net flux of photons from the conduction band reservoir to the intermediate band reservoir must first be set equal, or as near to equal as

numerically possible, to the net flux of photons from the intermediate band reservoir to the valence band reservoir. Additionally, in situations where it is necessary to evaluate radiation flux whose chemical potential is very near to the absorption edge of the matter, numerical computation of the Bose-Einstein integrals becomes very slow and subject to large numerical errors because of the need to evaluate near a singularity.

The approach given herein, transforms the Bose-Einstein integral into a linear combination of incomplete Riemann zeta integrals (IRZI). The integrands of each of the IRZI are functions of a single dummy variable,  $x$ . For each IRZI two LUT are created: one denoting intervals by which a composite integration is pre-computed across the numerical domain,  $\mathcal{D}_x$ , of the dummy variable  $x$ ; and a second recording the computed values of the IRZI whose limits of integration are held by the first LUT. In those cases where calculating flux requires evaluating the Riemann zeta integrands for  $x$  outside of  $\mathcal{D}_x$  limiting approximations to the integrands are employed; specifically, approximations where the component due to  $x$  outside of  $\mathcal{D}_x$ , is analytic and calculable. In those cases where calculating flux requires evaluating the Riemann zeta integrands for  $x$  inside of  $\mathcal{D}_x$  the high-precision LUT are employed; such that over a large portion of the interval between the limits of integration, summation replaces numerical integration. The use of the limiting approximations and LUT allows for precise and rapid computation of flux.

The organization of the paper is as follows: the next section presents the details of this method, the third section shows means by which the precision of the method has been verified, and the fourth section presents efficiency limit calculations for the IBSC where the solar concentration is intermediate between the extrema.

## 2 CALCULATION OF FLUX

To calculate flux rapidly and precisely an integral is sought such that its integrand is a function of a single dummy variable and its limits of integration allow it to be a proper definite integral. In order to avoid accruing numerical error, the limitations of the computer arithmetic must be considered with respect to the integrands. In regions where there is large floating-point error, appropriate limiting functions must be employed to approximate the

integrands. Finally, consideration must be given to the generation of the LUT.

2.1 A form suitable for numerical computations

The integral describing photon flux,  $F_p$ , derives from the emissivity of the matter that the photons are interacting with, the density of states, and the Bose-Einstein statistics. The canonical form of the flux is given as:

$$F_p(E_A, E_B, T, \mu) = \begin{cases} \frac{2\pi}{c^2 h^3} \frac{E_B^{E_A}}{E_A} \frac{E^P dE}{\exp\left(\frac{E-\mu}{kT}\right) - 1}, & \text{for } \mu < E_A; \\ 0, & \text{for } \mu \geq E_A; \end{cases}$$

**Eq. 1**

where  $E_B$  and  $E_A$  are the upper and lower limits of the emissivity of the solid respectively,  $\mu$  is the chemical potential of the radiation,  $T$  is the surface temperature of the matter,  $c$  is the speed of light,  $h$  is Planck's constant,  $k$  is Boltzmann's constant and  $P$  takes the values 2 or 3 for the calculation of particle flux or energy flux respectively [8]. In future expressions for flux, it is understood that the condition  $\mu < E_A$  holds so that the flux is non-zero.

The first step in creating LUT, which expedite the rapidity and precision of flux calculations, is to transform **Eq. 1** into a form whose integrands are functions of unitless, dummy variables. By the following substitution,  $y = (E - \mu)/kT$ , **Eq. 1** is rewritten as a linear combination of IRZI:

$$F_p = \sum_{p=1}^{p+1} a_{p-1} \int_{(E_A - \mu)/kT}^{(E_B - \mu)/kT} \frac{y^{p-1} dy}{\exp(y) - 1}; \quad \text{Eq. 2}$$

where  $a_{p-1}$  may be determined from carrying through the algebra. Though the integrands of **Eq. 2** are a function of a unitless dummy variable, the form of **Eq. 2** is not always suitable for obtaining high precision results. Such is the case when the upper limit of the emissivity tends towards infinity, which is the case in the majority of efficiency limit calculations. In such circumstances, the forms given by **Eq. 1** and **Eq. 2** become improper integrals. Thus, the numerical integration tends to become arbitrary, as the following question must be answered: Just how large is infinity? With some authors, for example, choosing 6 eV [6]? In order to surmount this problem the substitution  $x = 1/y$  is employed and thus flux is re-written as:

$$F_p = \sum_{p=1}^{p+1} a_{p-1} \int_{kT/(E_B - \mu)}^{kT/(E_A - \mu)} \frac{dx}{x^{p+1} \left[ \exp\left(\frac{1}{x}\right) - 1 \right]}. \quad \text{Eq. 3}$$

The form of **Eq. 3** is superior to the two previous forms because it allows for the construction of LUT and it avoids the difficulty of evaluating improper integrals. An additional benefit of **Eq. 2** and **Eq. 3** is that the individual integrals (for  $p$  a positive integer greater than one) may be compared with closed form expressions of the Riemann zeta function, thus allowing checks on the precision of the method.

2.2 The limitations of computer arithmetic

Computer arithmetic further complicates the precise computation of flux. When  $x$  is small, one must guard against underflow errors when evaluating the Riemann zeta integrands. For comparison, when  $E$  of **Eq. 1** is

large, one must guard both against underflow and round-off errors. Further, when  $x$  is large the floating-point error caused by the subtraction in the denominator causes the integrands to oscillate with  $x$ , until finally one-over-zero errors occur. This may be seen clearly by plotting the relative error between the integrands and a limiting approximation to the integrands. Figure 1 illustrates for the case  $p=2$  that the Riemann integrand of **Eq. 3** begins to oscillate with  $x$  but that the integrand may be approximated by a limiting expression given in **Eq. 5**. For comparison, when  $\mu$  nears  $E_A$ , the same phenomenon is observed for the Bose-Einstein integrands. As  $x$  increases a bit beyond  $1e7$ , the relative error between the two integrands stops decreasing and begins to oscillate with larger and larger amplitude. Thus, for all the Riemann integrals, there is a fixed domain of  $x$ ,  $\mathcal{D}_x$ , such that the integrands are both computable and stable. The limits of this domain largely depend upon the machine precision of the microprocessor, yet, some judgment is necessary as to the location of the upper cutoff of the domain. The authors have found that for a machine precision of order  $1e-16$ , that  $\mathcal{D}_x = [1.41e-3, 1.00e7]$  is suitable for all the orders of the IRZI that are of interest ( $p = 1, 2, 3, 4$ ). The limits of this numerical domain derive purely from the constraints of the computer arithmetic, as opposed to considerations regarding the spectrum of a given radiation of interest.

In those cases where there is a contribution to the flux from outside the boundaries of  $\mathcal{D}_x$ , limiting expressions must be used to calculate that contribution. The authors recommend the use of  $\hat{F}_p^{(LOW)}$  and  $\hat{F}_p^{(HIGH)}$  to calculate that contribution if  $kT/(E_B - \mu) < \min(\mathcal{D}_x)$  and if  $kT/(E_A - \mu) > \max(\mathcal{D}_x)$  respectively, where:

$$\hat{F}_p^{(LOW)} = \sum_{p=1}^{p+1} a_{p+1} \int_{kT/(E_B - \mu)}^{\min(\mathcal{D}_x)} \frac{dx}{x^{p+1} \exp\left(\frac{1}{x}\right)}, \quad \text{and} \quad \text{Eq. 4}$$

$$\hat{F}_p^{(HIGH)} = \sum_{p=1}^{p+1} a_{p+1} \int_{\max(\mathcal{D}_x)}^{kT/(E_A - \mu)} \frac{dx}{x^p}. \quad \text{Eq. 5}$$

Note that **Eq. 4** and **Eq. 5** are both analytic and thus can be expressed in a closed-form, which further augments both the precision and the speed of computation, as numerical integration is unnecessary. In addition to their utility in approximating flux outside the bounds of  $\mathcal{D}_x$ , **Eq. 4** and **Eq. 5** may be used to gauge the accuracy of computations while debugging software, and even, in some cases, to approximate the flux across the whole limit of integration,  $E_A$  to  $E_B$ , as will be seen in section 3.

2.3 The look-up-tables for Riemann zeta integrals

Each of the Riemann integrals is associated with two LUT: one containing increasing values of  $x$ , beginning with  $\min(\mathcal{D}_x)$  and ending with  $\max(\mathcal{D}_x)$ ; and a second recording the computed values of the IRZI between two successive entries in the first LUT. For example, in calculating the particle flux in a situation such that  $\min(\mathcal{D}_x) < E_A < E_B < \max(\mathcal{D}_x)$ , the operations given in **Eq. 6** are performed, where  $x_n^{(p)}$  is the smallest value in the first LUT associated with the  $p^{\text{th}}$  Riemann zeta integral greater than  $kT/(E_B - \mu)$ ,  $x_N^{(p)}$  is the largest value in the

first LUT associated with the  $p^{\text{th}}$  Riemann zeta integral less than  $kT/(E_A - \mu)$ , and all the integrals in the inner summation are pre-computed and recorded in the second LUT associated with the  $p^{\text{th}}$  Riemann zeta integral.

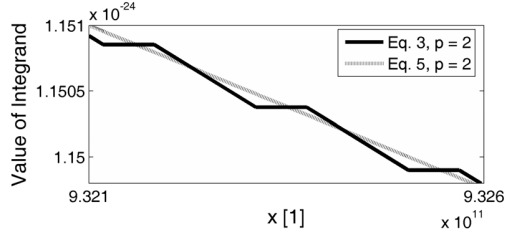


**Figure 1:** For large  $x$ , evaluation of Riemann zeta integrands is subject to round-off errors that are caused by the denominator terms. In these cases, the integrands may be approximated by limiting functions such as those given in Eq. 5.

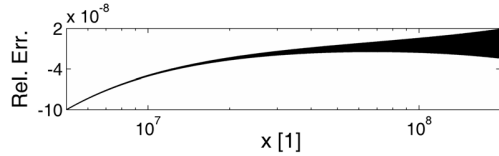


**Figure 2:** As  $x$  increases beyond  $1e7$ , the relative error between the integrands of Eq. 3 and Eq. 5 begins to oscillate with increasing amplitude. This is true for  $p = 1, 2, 3, 4$ . This figure shows  $p = 2$ .

Pre-computing LUT in the manner of Eq. 6 not only speeds up calculations during run time, but, in general provides more precise results. The reason being is that numerical integration routines are almost exclusively based upon interpolation polynomials and the integrands of the Riemann zeta integrals must be interpolated with polynomials of very large order. Thus, in general, numerical integration routines will have a difficult time maintaining both precision and rapidity, especially over large intervals [7]. Therefore, the method that the authors adopt is to generate LUT by composite integration across  $\mathcal{Q}_x$ , where  $\mathcal{Q}_x$  has been cut into roughly logarithmically spaced intervals. Within each logarithmically spaced interval the values of the incomplete Riemann integrals are computed with Simpson's adaptive quadrature method. All calculations are done with a machine precision of order  $1e-16$ .

#### 2.4 Additional remarks

With the use of this method, under most circumstances, computing the flux requires that a numerical integration routine be called  $2*(P+1)$  times; which is compared to a single call if using the Bose-Einstein integral of Eq. 1. However, with this method, the integration limits will be very small due to the complementary usage of LUT. The results of the  $2*(P+1)$  calls to the numerical integration routine are added to the results of  $P+1$  calls to LUT.

### 3 VERIFICATION OF HIGH PERFORMANCE METHOD

The numerical software that implements this method is benchmarked for precision by a number of means.

These include comparisons between the Riemann zeta functions, and previously recorded values for solar cell limiting efficiencies from the literature.

Firstly, the fact that the complete Riemann zeta integrals for positive integers greater than 1 are given in closed form allows for a comparison that provides conclusive indication of the precision of the combination of LUT and limiting expressions. For  $p = 2, 3, 4$  the simulator showed an absolute error of order  $1e-14$  such that the computed value was greater than the closed form expression. The computational package is also benchmarked against a number of efficiency limit results for the single  $p$ - $n$  junction solar cell and the IBSC.

$$F_2(E_A, E_B, T, \mu) = \sum_{p=0}^2 a_p + \sum_{k=n}^{N-1} \int_{x_k^{(p)}}^{x_{k+1}^{(p)}} \frac{dx}{x^{p+2} \left[ \exp\left(\frac{1}{x}\right) - 1 \right]} + \int_{x_n^{(p)}}^{x_N^{(p)}} \frac{dx}{\frac{kT}{E_B - \mu} x^{p+2} \left[ \exp\left(\frac{1}{x}\right) - 1 \right]}$$

**Eq. 6**

In order to judge the precision of the numerical package, results were compared with previous results obtained by the literature. Under maximum solar concentration, a solar surface temperature,  $T_s$ , of 5762 K, and a planetary surface temperature,  $T_p$  of 288 K, the efficiency limit of the single junction solar cell (SJSC) is calculated as 40.7% when the bandgap,  $E_g$ , is 1.06 eV. This compares favorably to the results of De Vos (40.8% for  $E_g = 1.15$  eV) [8]. It is worth noting that under these conditions if Eq. 4 is used to approximate the solar cell flux over the complete limit of integration,  $x = [0, kT_s/E_g]$  (where  $\mu = E_g*(1-T_p/T_s)$ ) [8], which is justified because for  $E_g = E_A$  of order 1 eV the integrand of Eq. 3 is dominated by the exponential term, then the solar cell particle flux may be approximated analytically. The resultant value will be slightly larger than what would be obtained from numerical calculations using Eq. 3 because, for all values of  $x$ , the denominator of Eq. 4 is greater than the denominator of Eq. 3. Thus a ceiling is obtained, whereby any computed efficiency above this ceiling is patently invalid. The efficiency limit computed in this manner, for the identical conditions stated in the beginning of this paragraph, establishes a ceiling of 40.8%. Using the same temperatures as listed above, but with a solar concentration of  $x1$ , the optimum efficiency is computed as 31.0% when  $E_g = 1.26$  eV. These results compare favorably with the work of De Vos, who records the identical efficiency when  $E_g = 1.30$  eV [8]. The numerical package is also benchmarked on the efficiency limit of a SJSC at full concentration but with  $T_s = 5759$  K and  $T_p = 300$  K. The results of such calculations provide an efficiency limit of 40.6% at  $E = 1.06$  eV, which compare favorably to previously reported results under identical conditions: 40.7% at  $E_g = 1.06$  eV [9].

Finally, the software package has been benchmarked against previous calculations of the IBSC. The numerical software obtains an efficiency limit for the

IBSC of 63.2%, which is obtained when the effective band gap between the conduction band and valence band is 1.95 eV and the effective band gap between the intermediate band and valence band is 0.71 eV. This result compares exactly with the result of Luque and Martí [6]. Additionally, under 1-sun illumination the simulator calculates an optimum efficiency of 46.8%, which is obtained when the effective band gap between the conduction band and valence band is 2.40 eV and the effective band gap between the intermediate band and valence band is 0.92 eV. This result again compares favorably with the previously reported optimized efficiency of 46.0%, which is reported to occur when the effective band gap between the conduction band and valence band is 2.43 eV and the effective band gap between the intermediate band and valence band is 0.93 eV [6].

The next section presents new results for the optimized efficiency of IBSC for a number of solar concentrations intermediate between the two extreme values.

#### 4 CALCULATION OF OPTIMIZED EFFICIENCY OF IBSC AT VARIOUS CONCENTRATIONS

The numerical package is used to compute the optimized efficiencies of SJSC and IBSC for a number of solar concentrations intermediate between the two extreme values. This task is accomplished by adjusting parameters so that the product of the net particle flux absorbed by the IBSC and the quasi-Fermi level separation between the conduction band and valence band,  $\mu_{CV}$  is maximized. Yet, the net flux selectively absorbed between the conduction band and intermediate band reservoirs,  $\dot{N}_{CI}$ , must be equal to the flux selectively absorbed between the intermediate band and valence band,  $\dot{N}_{IV}$ . The difference between  $\dot{N}_{CI}$  and  $\dot{N}_{IV}$ , for a given value of  $\mu_{CV}$ , is a function of the quasi-Fermi level separation between the intermediate band and valence band,  $\mu_{IV}$ . In obtaining the results presented herein, two values of the chemical potential,  $\mu_{IV,1}$  and  $\mu_{IV,2}$  were sought so that two conditions were met within specified tolerances. The conditions and their respective tolerance are given as:

$$\left| \left[ \dot{N}_{CI} - \dot{N}_{IV} \right] (\mu_{IV,1}) - \left[ \dot{N}_{CI} - \dot{N}_{IV} \right] (\mu_{IV,2}) \right| < 1 \times 10^{10} \frac{\#}{\text{m}^2 \text{s}},$$

$$\text{and } \left| \frac{\mu_{IV,2} - \mu_{IV,1}}{\mu_{IV,1}} \right| < 1 \times 10^{-4}.$$

The tolerances of the above two conditions are chosen through a process of trial and error, bearing in mind the trade-offs between precision and speed of computation. Efficiency limit calculations are found to be more sensitive to the second condition than to the first condition. Further, at the specified tolerance for the second condition, the calculated efficiency saturates with respect to a further reduction in this tolerance, whereas the speed of computation continues to increase.

The results of such calculations are reproduced graphically in Figure 3 for both the IBSC and SJSC. It may be seen from Figure 3 that the efficiency roughly increases logarithmically with increasing concentration for both the IBSC and the SJSC. Additionally, Table I records the relevant operating points for IBSC optimized for several different solar concentrations.

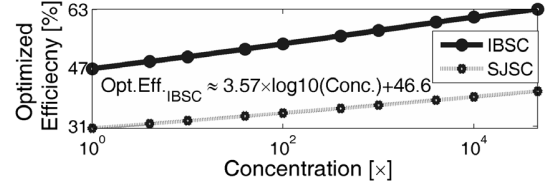


**Figure 3:** Optimized Efficiency as a function of solar concentration for the IBSC, SJSC and a three-junction serially-connected tandem solar cell. The result of a linear fit to the IBSC data is included.

	Concentration			
	x1	x10	x1,000	x46,296
Efficiency [%]	46.8	50.1	57.3	63.2
$E_{CV,OPT}$ [eV]	2.40	2.29	2.07	1.96
$E_{IV,OPT}$ [eV]	0.92	0.87	0.76	0.72
$\mu_{CV,OPT}$ [eV]	1.73	1.75	1.78	1.84
$\mu_{IV,OPT}$ [eV]	0.61	0.62	0.64	0.68

**Table I:** Simulated values of various parameters associated with an IBSC optimized for operation at four different solar concentrations.

#### 5 CONCLUSION

A method has been formulated to rapidly and precisely calculate particle flux and energy flux for efficiency limit calculations. The method transforms the canonical Bose-Einstein integral into IRZI, which enables the use of look-up-tables. The method has been benchmarked against previously reported results. In addition, the literature has been expanded by computing several optimized IBSC efficiencies for solar illuminations between the two extreme values. The results indicate a logarithmically increasing optimized efficiency with increasing solar concentration.

#### ACKNOWLEDGEMENTS

M.Y.L. thanks Dr. A. Martí for providing details of his numerical package, Dr. E. Croot for his suggestion of the Bernoulli generator, and for other mathematical assistance, and G. Levy for his technical mantra “do it systematically.” Both author give thanks to the U.S. National Renewable Energy Laboratory for their financial support through subcontract XAT-5-44277-01 administered by M. Symckos-Davies and R. McConnell.

- [1] V. Badescu, *Renewable Energy*, **30**, (2005) 211.
- [2] W. Shockley, H. Queisser, *Jour. App. Phys.* **32**, (1961), 510.
- [3] E.W. Ng, C.J. Devine, R.F. Tooper, *Math. Comp.*, **23**, (1969), 639.
- [4] E.W. Ng, C.J. Devine, *Math. Comp.*, **24**, (1970), 405.
- [5] O. Zobay, *Journal of Physics B: Atomic, Molecular and Optical Physics*, **37** (2004), 2593.
- [6] A. Luque, A. Martí, *Prog. Photo.*, **9** (2001), 73.
- [7] R. Burden, J. Douglas Faires, “*Numerical Analysis*,” ed. 6, Brooks/Cole Publishing Company, 1997, 199.
- [8] A. De Vos, “*Endoreversible Thermodynamics of Solar Energy Conversion*,” Oxford University Press, 1992, 96, 99.
- [9] G.L. Araujo, A. Martí, *Proc. 11 EC PVSEC*, Montreaux, (1992), 142.